Atom Indonesia

Journal homepage: https://atomindonesia.brin.go.id

Radial Sensitivity of the Nuclear Shell Structure at N=92

R. R. Swain[1], A. Anupam[1], P. Mohanty[1], K. K. Jena[2], S. K. Agarwalla[3], B. B. Sahu[1*]

[1]*Department of Physics, School of Applied Sciences, KIIT, Deemed to be University, Odisha 751024, India*
[2]*P. G. Department of Physics, Bhadrak Autonomous College, Bhadrak 756100, India*
[3]*P. G. Department of Physics, F.M. University, Balasore 756019, India*

ARTICLE INFO

Article history:
Received 24 June 2024
Received in revised form 14 August 2024
Accepted 28 August 2024

Keywords:
Improved mass formula
rms charge radius
Shell structures
Deformation

ABSTRACT

The nuclear ground-state properties of Samarium (Sm) isotopes are calculated and analyzed using an improved mass formula. The asymmetric energy term is consistently observed, separated into a volume and surface component. While distinctive signatures for certain isotopes remain elusive, the results show reasonable agreement with experimental data and well-established theoretical models such as the Relativistic-Continuum-Hartree-Bogoliubov (RCHB) and the Finite Range Droplet Model (FRDM). By utilizing a root-mean-square (rms) charge radius formula that incorporates both shell and deformation effects, the study provides new insights into the anomalous shifts observed in magic isotopes (N=82, N=126), as well as in N=92, 136, and 144 within the isotopic series of the "Sm" element.

INTRODUCTION

The rare earth element Samarium (Z=62) is distinguished by its unique combination of physical, chemical, and radioactive properties. It has emerged as a versatile element with applications in medical advancements [1], nuclear energy [2], and green chemistry [3,4]. Samarium-153 is one of the three radio-nuclides recently approved for the treatment of bone pain, while Samarium-149 [2], due to its excellent neutron absorption properties, is used in nuclear control rods. Recent studies [4] on a Samarium complex [Sm-bis (PYT) on boehmite nanoparticles] have also demonstrated its potential as a practical, stable, and recyclable nanocatalyst. Further research to explore more stable isotopes of this element is essential.

Nuclear masses, as one of the most fundamental aspects of nuclear physics, play a crucial role in understanding nuclear structures and provide insights into the behavior of nuclides far from the stability line. Over the years, several nuclear mass formulas have been developed to deepen the study of these properties. These include the classic Bethe-Weizsäcker (BW) type [5] as well as formulas based on macroscopic-microscopic models, such as the Finite Range Droplet Model (FRDM) [6], alongside microscopic approaches like the Hartree-Fock Bogoliubov method [7,8]. These formulas account for various factors, including isospin asymmetry, shell effects, deformations, and nuclear surface diffuseness. The macroscopic-microscopic mass formula, based on the Weizsäcker-Skryme (WS/WS*) models [9,10], predicts binding energies with an rms deviation of 0.323 MeV relative to 2,267 experimental masses. Additionally, the uncertainties of the Duflo-Zuker formula have also been extensively studied [11]. Mass formulas of the classic Bethe-Weizsäcker type, such as the one proposed by Spanier and Johansson [12], are particularly important for incorporating both shell and deformation energies. Further modifications [13] of the WS formula, have managed to reduce the rms deviation to 0.298 MeV, surpassing the 0.3 MeV threshold.

The complexity of nuclear structures far from the stability line, due to deformations and shell effects, necessitates the study of another key parameter closely influenced by these phenomena: the charge radius. Both the liquid drop model (LDM) charge radius and the root mean square (rms) charge radius play a crucial role in providing an accurate description of the nuclear structure and enhancing our understanding of nucleus-nucleus interactions [14]. Widely accepted microscopic

*Corresponding author.
E-mail address: bbsahufpy@kiit.ac.in
DOI: https://doi.org/10.55981/aij.2025.1491

models, such as the relativistic mean field (RMF) model [15] and the Skryme-Hartree-Fock-Bogoliubov (HFB) model [16], successfully reproduce charge radii for nuclei with Z>28, with rms deviation ranging from 0.0008 to 0.017 fm. Additionally, isospin-dependent phenomenological formulas [17-19] have been developed to describe both charge radii and rms charge radii accurately. However, despite their success, these formulas provide limited insight into the anomalous behavior of certain nuclides related to shell effects. Shell effects, associated with specific nucleon configurations and represented by neutron (N=2, 8, 20, 28, 50, 82, 126) and proton magic numbers (Z=2, 8, 20, 28, 50, 82), influence deformations in nuclides, especially far from the stability line. Thus, charge radius and rms charge radius formulas incorporating both shell and deformation terms are preferred for studies of these phenomena and their wider impact on nuclear structures.

METHODOLOGY

In this study, we employ the classic Bethe-Weizsäcker (BW) mass formula given by Spanier and Johansson [12] and the root mean square (rms) charge radius formula introduced by Wang and Li, in their rapid communication [20] to investigate the nuclear structures and ground-state characteristics of several Samarium isotopes within the heavy nuclide range (A=126 to A=216), far from the valley of stability.

The Liquid Drop Model (LDM)-based mass formula used here is an improvement on the formula originally proposed by Johansson [21], with its final form being a modification by Spanier and Johansson [12]. This formula represents a desired reduction in the number of parameters, contrasting with the trend at the time, where other mass formulas increased the number of free parameters for the sake of precision. The first part of the formula representing binding energies of the nuclides follows the conventional Weizsäcker type, comprising six terms as given by Eq. (1).

$$B.E.(Z,N) = a_1 A - a_2 A^{\frac{2}{3}} - a_3 \frac{z^2}{A^{\frac{1}{3}}} - a_4 \left(1 - \frac{a_5}{A^{\frac{1}{3}}}\right) \cdot \left(\frac{I^2 + a_6 I}{4A}\right) - a_7 I^4 - \frac{a_8}{A^{\frac{1}{2}}} \quad (1)$$

The first three terms represent the volume, surface, and coulomb energy, respectively, and are expressed through the simplest forms of the conventional type. Their corresponding mass coefficients are the free parameters a_1, a_2, and a_3, defined in Spanier and Johansson [12]. The value of a_3 is determined using a nuclear radius value of r_0=1.20 fm, which reproduces the coulomb energies accurately [12]. The asymmetric term, however, is modified by dividing it into volume and surface components, with the surface part including the Wigner term, I/A, where I = N – Z. An interim mass fit [12] to experimental data provides the optimal values for the parameters a_4, a_5, and a_6. For improved consistency with nuclear matter calculations, especially in line with recent studies based on the Bruechner-Hartree-Fock theory [22,23], another term of the form I^4 is included. The coefficient a_7 is selected to ensure proper alignment with similar theoretical calculations. The coefficient for the conventional pairing energy term, a_8 is obtained following the Bohr and Mottelson model [24]. The values of the mass coefficients are given in Table 1.

Table 1. Values of the free parameters in MeV.

a_1	a_2	a_3	a_4
16.1736	19.8092	0.72004	140.2839
a_5	a_6	a_7	a_8
2.0956	6.5205	2.7945×10-7	0 (E-E Nuclei) 11.9977 (Odd Nuclei) 23.9954 (O-O Nuclei)

The nuclear charge radius, one of the basic nuclear properties, can be described by the $A^{1/3}$ law, expressed as $\mathbf{R_c = r_0 A^{1/3}}$, where r_0 is the radius coefficient and A is the mass number. Shell effects, which refer to the arrangement of nucleons within energy levels or shells (analogous to electronic shells in atoms), significantly influence the overall shape and size of the nucleus. Nuclear deformation is another phenomenon strongly impacted by the shell structure of nuclides. The study of these phenomena, and their effects on parameters such as nuclear charge radius, requires formulas that account for both shell and deformation effects. The current formula (Eq. (2)) given by Wang and Li [20] incorporates both the shell correction and deformation terms, including quadrupole and hexadecapole deformations. Table 2 provides the values of coefficients used in Eqs. (2) and (3).

$$r_{ch} = \sqrt{\frac{3}{5}} R_c \left[1 + \frac{5}{8\pi}(\beta_2^2 + \beta_4^2)\right] \quad (2)$$

Where β_2 and β_4 represent the quadrupole and hexadecapole deformations, respectively, while R_c is expressed as a four-parameter formula for the charge radius given by Eq. (3).

$$R_c = r_0 A^{1/3} + r_1 A^{-2/3} + r_s I(1 - I) + r\Delta E/A \quad (3)$$

Table 2. Values of charge radius and rms charge radius formula parameters. The unit for r_d is $MeV^{-1}fm$ and the unit for other parameters is fm.

r_A	r_0	r_1	r_s	r_d
1.223	1.226	2.86	-1.09	0.99

The shell correction term (ΔE) and the deformation parameters (β_2, β_4) are derived from the WS3 model [13]. This model accounts for the mirror nuclei constraint and surface diffuseness, reducing the rms deviation of nuclear masses to 0.298 MeV relative to 2,149 measured masses. Our use of this model is validated by its success in investigations of shell corrections, deformations, neutron and proton drip lines, and shell gaps.

RESULTS AND DISCUSSION

The nuclear binding energy data obtained through computation of Eq. (1) for Samarium isotopes, ranging from A=120 to A=216, reveals a peak in binding energy per nucleon at neutron number N=82. This result is consistent with experimental data from the National Nuclear Data Center (NNDC) [25], as well as two widely accepted theoretical frameworks: the Relativistic-Continuum-Hartree-Bogoliubov (RCHB) [26] and the finite range droplet models (FRDM) [27], alongside the conventional BW formula [5]. The consistency revalidates the universally recognized concept of magic number and shell closure configuration, as shown in Fig. 1.

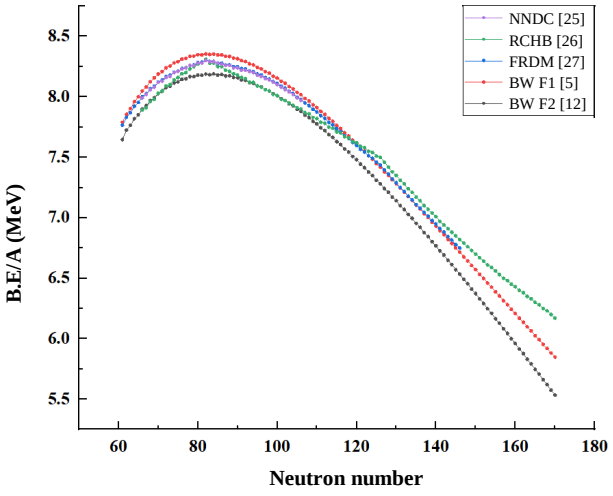

Fig. 1. Binding energies per nucleon as a function of neutron number for all studied Samarium nuclei. BW F1 denotes the conventional BW formula [5] and BW F2 denotes the modified formula given by Spanier and Johansson [12].

Further analysis of the enhanced stability of specific isotopes is conducted using several additional parameters. For the calculated binding energies, the two-neutron separation energy is defined using the RMF formalism [28] as given in Eq. (4),

$$S_{2n}(Z,N) = B.E.(Z,N) - B.E.(Z,N-2) \quad (4)$$

Subsequently, we also examine the oscillation in one-neutron separation energies [29], defined in Eq. (5),

$$D_n(Z,N) = (-1)^n[2B.E.(Z,N) - B.E.(Z,N-1) - B.E.(Z,N+1)] \quad (5)$$

and apply a three-point filter for the binding energy [30], as given by Eq. (6),

$$\Delta_{1n}^{(3)}B.E.(Z,N) = \frac{1}{2}(-1)^N[B.E.[Z,N+1] - 2B.E.(Z,N) + B.E.(Z,N-1)] \quad (6)$$

The two-neutron separation energies exhibit a sharp decline following neutron numbers N=82 and 126, based on the binding energies acquired from FRDM [27] and RCHB [26], as illustrated in Fig. 2. This observation aligns with the experimental data [25], reinforcing the characteristic energy shifts associated with established magic numbers.

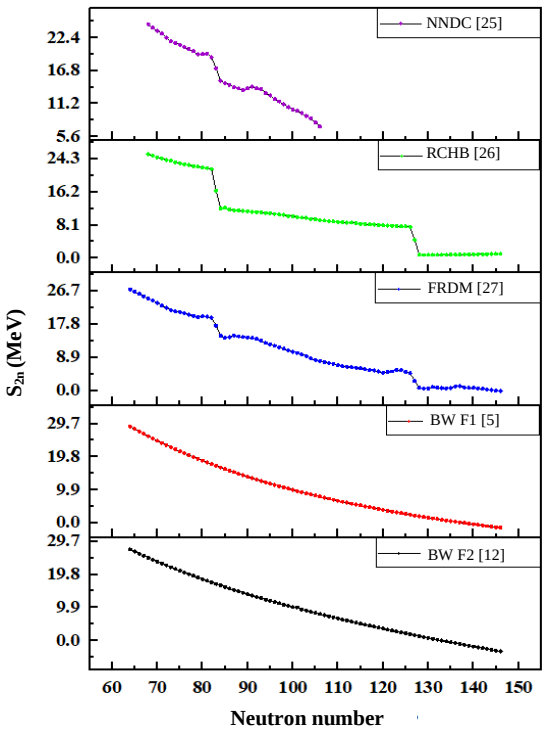

Fig. 2. Two neutron separation energies as a function of neutron number.

As shown in Figs. 3 and 4, the data for oscillation of one neutron separation energies and the three-point difference in binding energies, obtained from the NNDC [25] and the two theoretical models [26,27], provide valuable insights into the enhanced stability at the aforementioned neutron numbers. Additionally, anomalous shifts are observed at N=92 and N=94, suggesting potential for further investigation. However, no such shifts are evident in the calculated binding energies.

This signifies the absence of parameters that account for shell effects and nuclear deformations. The nuclear charge radius and rms charge radius formulas proposed by Wang and Li [20] address these limitations by incorporating both these factors. To visualize the impact of these two factors, a measured approach is required. First, we compute the rms charge radii of the aforementioned nuclides without considering either parameter followed by their successive incorporation. For rms charge radii without either parameter, we observe an exponential increase, consistent with the $A^{1/3}$ term of LDM, as observed in Fig. 5.

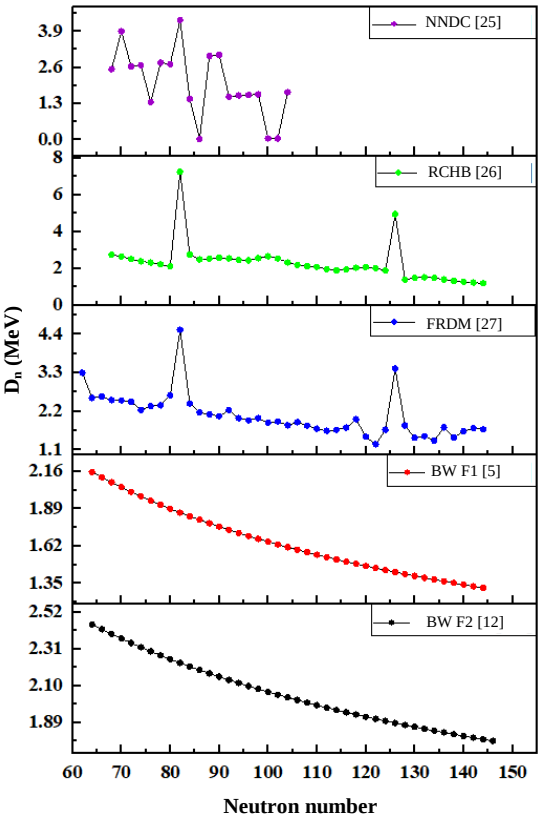

Fig. 3. One neutron separation energy difference as a function of neutron number.

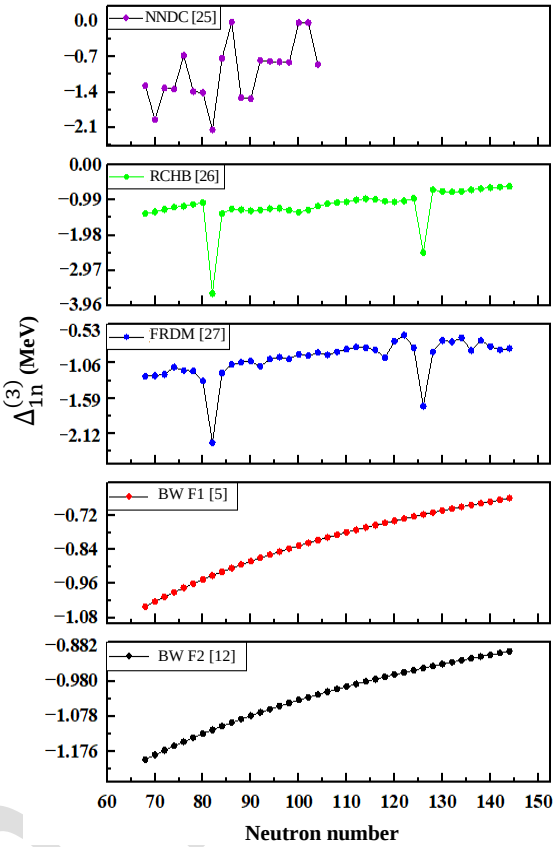

Fig. 4. Three-point difference in binding energies as a function of neutron number.

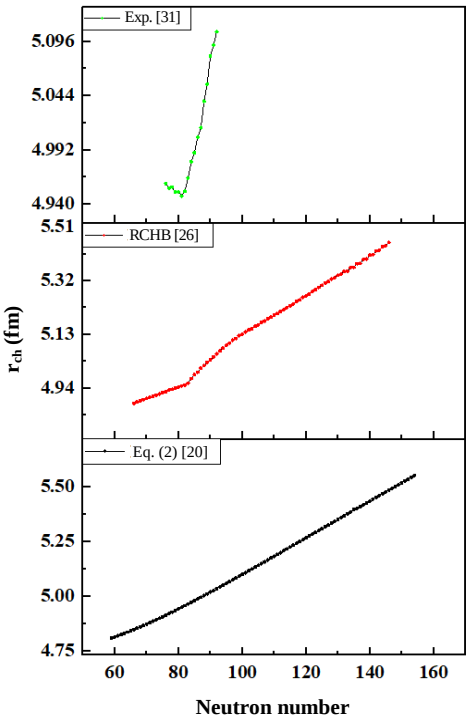

Fig. 5. rms charge radii as a function of neutron number for all studied Samarium nuclei without shell correction or deformation parameters.

The successive incorporation of each parameter yields expected results, with the charge radii displaying clear local minimum at the specified magic numbers. When both parameters are incorporated simultaneously, additional insights emerge, revealing enhanced stability at neutron numbers N=136 and N=144, as illustrated in Figs. 6, 7 and 8.

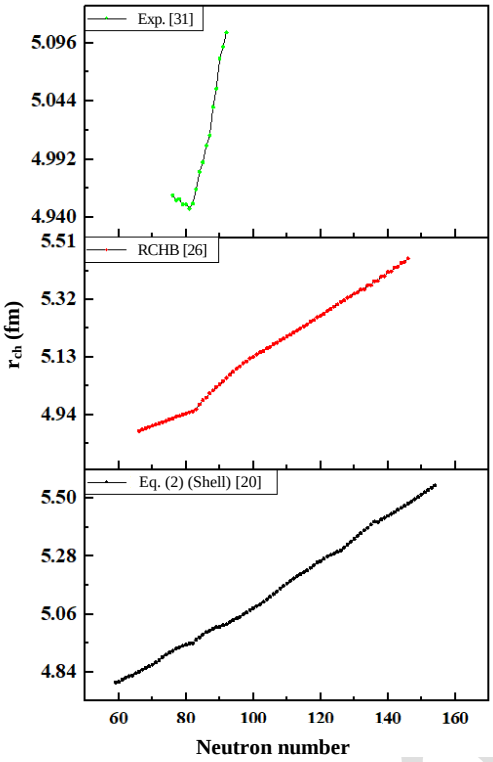

Fig. 6. rms charge radii with the shell correction parameter as a function of neutron number.

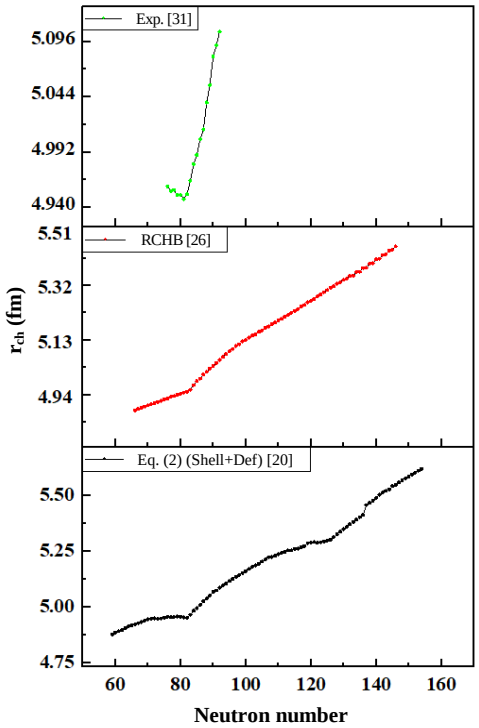

Fig. 7. rms charge radii (with the deformation parameter) as a function of neutron number.

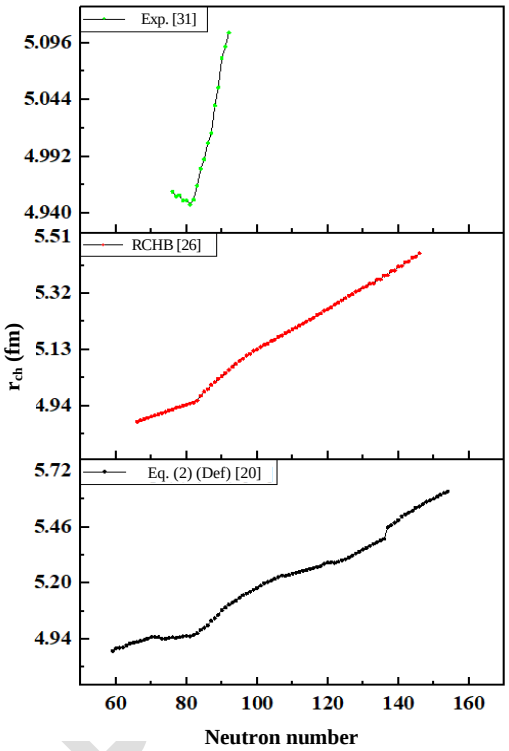

Fig. 8. rms charge radii (with both shell correction and deformation parameters) as a function of neutron number.

To further analyze these signatures of magicity and the other mentioned nuclides, we also apply the three-point filter [30] to the rms charge radii as defined in Eq. (7),

$$\Delta_{1n}^{(3)} r_{ch}(Z,N) = \frac{1}{2}(-1)^{N+1}[r_{ch}[Z,N+1] - 2r_{ch}(Z,N) + r_{ch}(Z,N-1)] \quad (7)$$

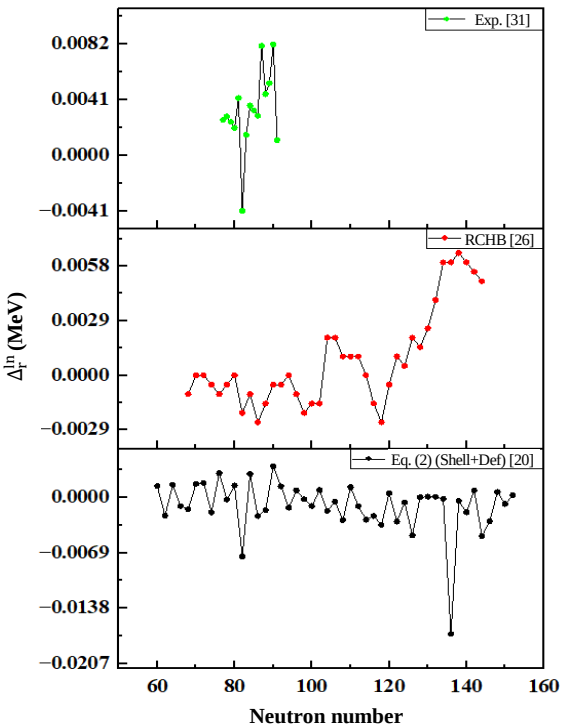

Fig. 9. Three-point charge radii difference as a function of neutron number.

All the calculations employing the current formula provide a reasonable agreement with the experimental data [31], emphasizing the robustness of the current theoretical model as observed in Fig. 9.

CONCLUSION

Nuclear structures and the phenomena that influence it remain key areas of research in nuclear physics. As studies on the discovery of novel stable isotopes for experimental and practical applications accelerate, our work re-affirms the significance of two crucial factors, shell effects, and nuclear deformations, in the accurate determination of nuclear ground state properties. The rms charge radii calculations, incorporating shell and deformation terms either successively or concurrently, reveal signatures of enhanced nuclear stability at neutron numbers N=92, N=136, and N=144, in addition to the well-established magic isotopes. Similar studies on nuclear structure, though applied to different isotopic chains, have also been carried out using RMF formalism [32], providing complementary perspectives on stability trends. However, the LDM based mass formula offers limited insight in this regard, suggesting opportunities for further investigations.

ACKNOWLEDGMENT

This work was made possible by the computational infrastructure provided by KIIT, Deemed to be University, and the authors gratefully acknowledge this support.

AUTHOR CONTRIBUTION

The primary contributor, Ratan R. Swain, declares, that all authors have read and approved the final version of the paper.

REFERENCES

1. A. I. Nabeel, Tumor Biol. **42** (2020) 1.
2. O. Moreira, Ann. Nucl. Energy **83** (2015) 87.
3. Y. Cheng, H. Nan, Q. Li *et al.,* ACS Sustain. Chem. Eng. **8** (2020) 13908.
4. P. Moradi, T. Kikhavani and Y. A. Tyula, Sci. Rep. **13** (2023) 5902.
5. H. A. Bethe, Phys. Rev. **50** (1936) 332.
6. P. Möller, A. J. Sierk, T. Ichikawa *et al.,* At. Data Nucl. Data Tables **109-110** (2016) 1.
7. J. Geng and W. H. Long, Phys. Rev. C **105** (2022) 034329.
8. Y. el Bassem and M. Oulne, Nucl. Phys. A **957** (2017) 22.
9. N. N. Ma, H. F. Zhang, X. J. Bao *et al.*, J. Phys. G: Nucl. Part. Phys. **42** (2015) 095107.
10. M. Liu, Y. Gao and N. Wang, Chin. Phys. C **41** (2017) 114101.
11. C. Qi, J. Phys. G: Nucl. Part. Phys. **42** (2015) 045104.
12. L. Spanier and S. A. E. Johansson, At. Data Nucl. Data Tables **39** (1988) 259.
13. N. Wang, M. Liu, X. Wu *et al.*, Phys. Lett. B **734** (2014) 215.
14. A. S. Umar, C. Simenel and K. Godbey, Phys. Rev. C **104** (2021) 034619.
15. R. An, S. S. Zhang, L. S. Geng *et al.,* Chin. Phys. C **46** (2022) 054101.
16. R. Shou, X. Yin, C. Ma *et al.*, Phys. Rev. C **106** (2022) L061304.
17. T. Naito, X. Roca-Maza, G. Colò *et al.,* Phys. Rev. C **106** (2022) L061306.
18. R. An, X. Jiang, N. Tang *et al.,* Phys. Rev. C **109** (2024) 064302.
19. J. Q. Ma and Z. H. Zhang, Chin. Phys. C **46** (2022) 074105.
20. N. Wang and T. Li, Phys. Rev. C **88** (2013) 011301.
21. S. A. E. Johansson, Ark. Fys. **22** (1962) 414.
22. S. Wang, Q. Zhao, P. Ring *et al.*, Phys. Rev. C **103** (2021) 054319.
23. W. H. Long, J. Geng, J. Liu *et al.*, Commun. Theor. Phys. **74** (2022) 097301.
24. H. G. Ganev, Eur. Phys. J. A **57** (2021) 181.
25. NuDat, Binding Energy per Nucleon of Sm Isotopes, https://www.nndc.bnl.gov/nudat/. Retrieved in January (2024).
26. X. W. Xia, Y. Lim, P. W. Zhao *et al.*, At. Data Nucl. Data Tables **121-122** (2018) 1.
27. P. Möller, M. R. Mumpower, T. Kawano *et al.*, At. Data Nucl. Data Tables **125** (2019) 1.
28. R. R. Swain, B. B. Sahu, P. K. Moharana *et al.*, Int. J. Mod. Phys. E **28** (2019) 1950041.

29. B. A. Brown, J. Phys. Conf. Ser. 580 (2015) 012016.
30. Á. Koszorús, X. F. Yang, W. G. Jiang *et al*., Nat. Phys. **17** (2021) 439.
31. I. Angeli and K. P. Marinova, At. Data Nucl. Data Tables **99** (2013) 69.
32. M. Das, K. C. Naik, N. Biswal *et al*., Atom Indones. **48** (2022) 115.